Geomorphology 123 (2010) 34–45

Contents lists available at ScienceDirect

Geomorphology

journal homepage: www.elsevier.com/locate/geomorph

Tectonic geomorphology of the southern Sierra Nevada Mountains (California): Evidence for uplift and basin formation

Andrea M. Figueroa, Jeffrey R. Knott *

Department of Geological Sciences, California State University Fullerton, Fullerton, CA 92834, United States

ARTICLE INFO

Article history:
Received 28 April 2008
Received in revised form 4 June 2010
Accepted 7 June 2010
Available online 20 June 2010

Keywords:
Tectonic geomorphology
Geomorphic indices
Sierra Nevada Mountains
Kern River

ABSTRACT

Hypotheses regarding uplift of the Sierra Nevada Mountains (Sierra), California, USA, vary from a single slowly tilting block to rapid Pliocene and/or Quaternary uplift in the south exclusively. To test these hypotheses, we examined geomorphic indices of the western Sierra. We interpret longitudinal profiles of the larger westerly flowing rivers, mountain front sinuosity, valley floor-to-width to height ratio, and relief ratio to show that relative tectonic activity is greater in the southern Sierra near the Kern River Gorge fault. The Sierra range crest profile indicates that the increased tectonism is related to more recent uplift in the southern Sierra. Only westward migration of Basin and range extension is consistent with the locus of uplift in the southern Sierra. We hypothesize that the Sierra topography is the result of Pliocene delamination-related uplift in the central Sierra and post-Pliocene interaction of the San Andreas, Garlock, and Sierra Nevada Frontal fault zones.

1. Introduction

Several different hypotheses for the style and mechanism of late Cenozoic Sierra Nevada Mountains, California, USA (Sierra) surface uplift have been proposed (Huber, 1981; Unruh, 1991; Wakabayashi and Sawyer, 2001; Stock et al., 2004). Mechanisms range from uniform uplift (Wakabayashi and Sawyer, 2001), Basin and Range extension (Niemi, 2003), lower crust and upper mantle delamination (Saleeby and Foster, 2004) to climatically driven denudation (Small and Anderson, 1995). Taken at face value, these hypothesized mechanisms should produce differing rates and amounts of range uplift (Fig. 1) and must account for the anomalous topography in the Kings–Kaweah region (Saleeby and Foster, 2004) and explain basin formation in the southern San Joaquin Valley (Bartow, 1991).

Geomorphic studies have focused on the topographic expression of specific aspects of late Cenozoic Sierra tectonic geomorphology such as Kings River incision (Stock et al., 2004), geomorphic change along the eastern mountain front (e.g., Brocklehurst and Whipple, 2002), or incision of northern rivers (Huber, 1981; Unruh, 1991). An underlying assumption of late Cenozoic Sierran tectonic geomorphology is that the normal-slip Owens Valley Frontal fault generates an active mountain front to the east, whereas the western range front is passive. However, the premise of a passive western mountain front overlooks or was developed prior to recognition of (1) the geomorphically youthful Kern River Gorge fault in southwestern Sierra (Fig. 1; Nadin and Saleeby, 2010); (2) the post-Pliocene incision of the westward-flowing Kings River (Stock et al., 2004); (3) the mantle delamination and accompanying mantle drip and anomalous topography at the western range front (Fig. 1; Saleeby and Foster, 2004). In addition, no geomorphic study has examined the geomorphic variation of the Sierra with latitude due to the lack of adequate paleo-channel indicators south of the San Joaquin River (Wakabayashi and Sawyer, 2001).

In this study, we apply geomorphic indices to the western mountain front and west-flowing rivers of the Sierra. We chose geomorphic indices based on their likelihood to record perturbations (e.g., mountain front sinuosity; Burbank and Anderson, 2001) or reach equilibrium (e.g., longitudinal profiles and valley floor width to height ratios of trunk streams; Bull, 1984) over late Cenozoic time scales. These types of geomorphic indices are most commonly applied to mountain fronts with a well-defined bounding fault; however, the western Sierra mountain front is hypothesized to have tectonically generated topography (Saleeby and Foster, 2004) and rivers responding to mountain uplift and base level drop (Stock et al., 2004). When combined, geomorphic indices may distinguish between areas with varying uplift rates along the length of a particular mountain range (e.g., Bull and McFadden, 1977; Wells et al., 1988).

We examine the western Sierra mountain front in an attempt to detect tectonic geomorphic changes related to the fault-bounded southwestern area and the mantle delamination and drip in the west-central region (Saleeby and Foster, 2004; Stock et al., 2004) as well as other proposed mechanisms of tectonic uplift. Advantages to examining the western drainages are that (i) the large rivers with

* Corresponding author. Department of Geological Sciences, 800 N. State College Blvd. California State University Fullerton, Fullerton, CA 92834-6850, United States. Tel.: +1 657278 5547; fax: +1 657278 7266.
E-mail address: jknott@fullerton.edu (J.R. Knott).

0169-555X/$ – see front matter © 2010 Elsevier B.V. All rights reserved.
doi:10.1016/j.geomorph.2010.06.009

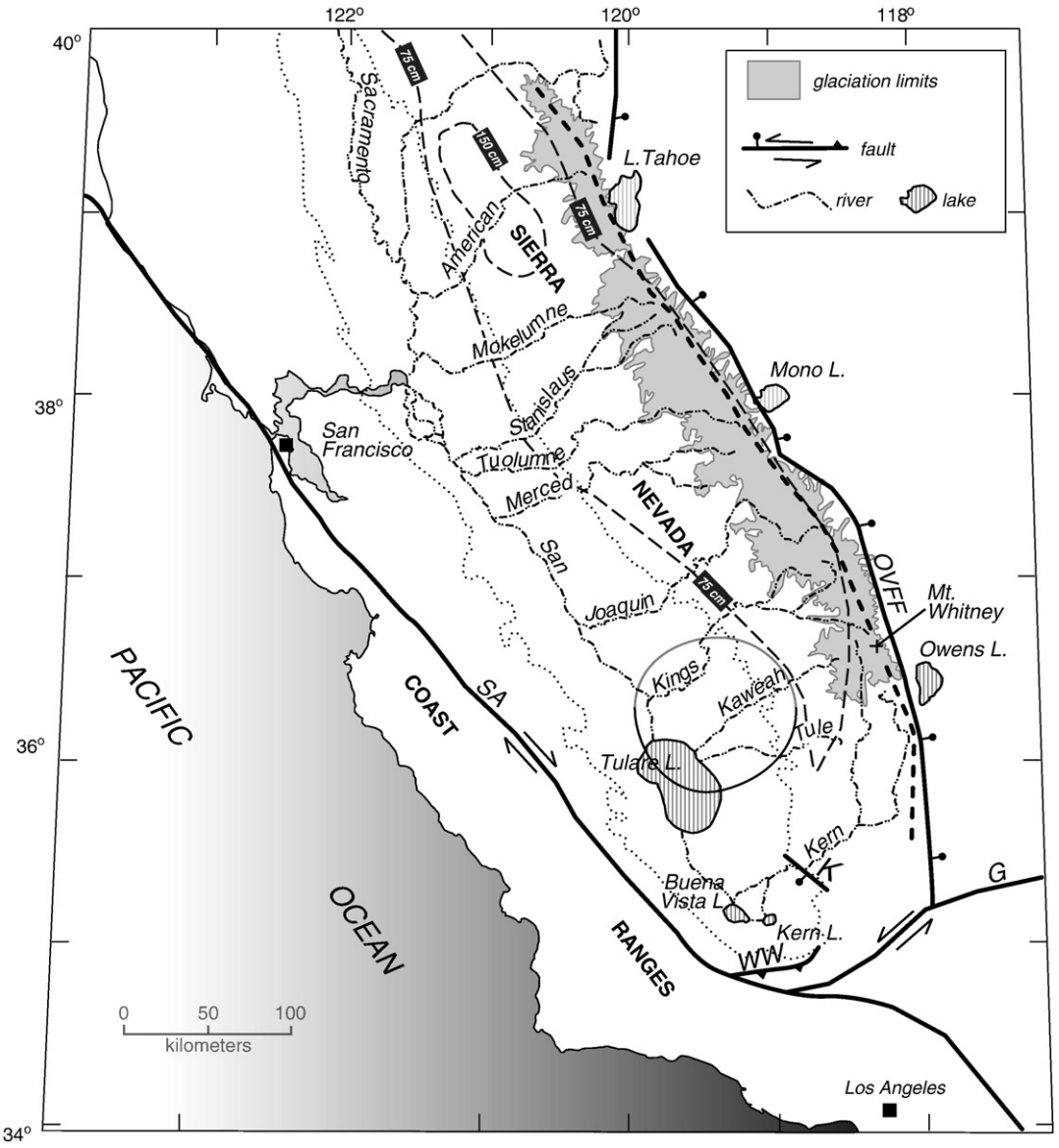

Fig. 1. Sierra Nevada and vicinity (after Atwater et al., 1986). Dotted line is edge of San Joaquin and Sacramento River valleys. Long dash line is approximate location of Sierra Nevada crest and range crest profile. Mt. Whitney is the highest point in the Sierra. The circular area is the approximate location of the mantle drip (Saleeby and Foster, 2004). Major faults are San Andreas (SA), Garlock (G), Owens Valley frontal fault (OWFF), White Wolf (WW) and Kern River Gorge (K). Ball and bar and barb are on hanging wall for normal and thrust faults, respectively. Strike-slip motion shown by arrows. The precipitation contours of 150 cm/yr and 75 cm/yr are generalized from National Atlas of the United States (2010). Limits of glaciation are the Tahoe stage of Blackwelder (1931) taken from Atwater et al. (1986).

their greater stream power will reach equilibrium more rapidly than tributary drainages and therefore will only record sustained uplift or base level changes and (ii) only the headwaters of the rivers is impacted by late Pleistocene glaciations (Fig. 1) whereas the eastern drainages were eroded by late Pleistocene glaciers that extended onto the adjacent piedmont.

2. Regional setting

Thermochronologic studies have shown that an ancestral Sierra was uplifted (i.e., surface uplift) during the late Cretaceous to earliest Cenozoic, followed by much lower rate of uplift in the middle to late Cenozoic (Dumitru, 1990; House et al., 1997, 1998, 2001; Cecil et al., 2006). This two-phase uplift history is seen throughout the Sierra from the Kern River to the American River (Cecil et al., 2006). Late Cretaceous elevations were high enough to generate a rain shadow (Poage and Chamberlain, 2002) with an estimated crest elevation range of <1500 m (Clark et al., 2005). The second uplift phase in the late Cenozoic started between 5 and 10 Ma (Huber, 1981; Graham et al., 1988; Unruh, 1991; Wakabayashi and Sawyer, 2001 Clark et al., 2005) and was dominated by westward tilting. Several studies have concluded that the total surface uplift during this second phase was approximately 950–2500 m (Huber 1981; Unruh, 1991; Wakabayashi and Sawyer, 2001; Clark et al, 2005). Through the years, a number of studies proposed a variety of tectonic mechanisms to produce this late Cenozoic uplift and the present elevation of the mountain range. Different amounts of late Cenozoic uplift, both spatially and temporally (Fig. 2), are predicted by the hypothesized uplift mechanisms.

The most frequently cited mechanism is westerly tilting attributed to normal faulting along the east side of the Sierras (Huber, 1981; Unruh, 1991). Based on river incision and sedimentation data, Huber (1981) proposed that the Sierras experienced uniform westward tilting of the entire Sierra from north to south (Fig. 2e) because of uplift on the Owens Valley Frontal fault. Wakabayashi and Sawyer (2001) supported this hypothesis by noting that relatively uniform uplift rates inferred from river incision are seen from the Yuba River

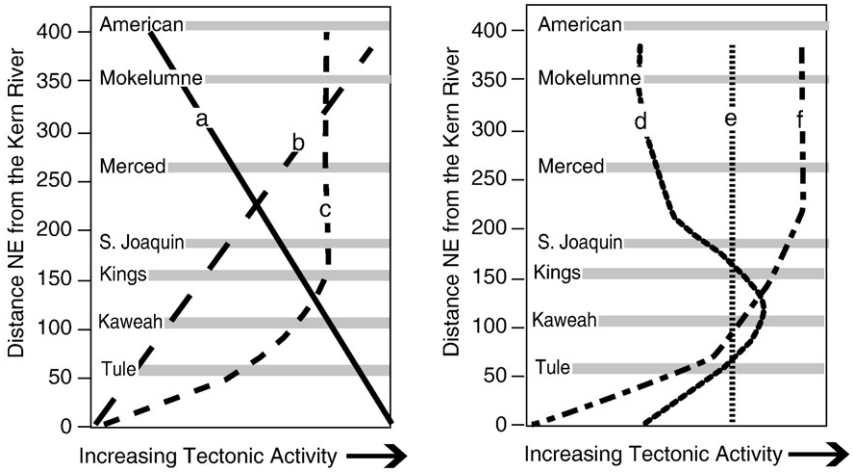

Fig. 2. Hypothetical relations between tectonic geomorphic indices and differing tectonic uplift scenarios: (a) delamination caused by Basin and Range extension (Ducea and Saleeby, 1998; Liu and Shen, 1998; Manley et al., 2000; Niemi, 2003); (b) northward migration of the Mendicino triple junction (Crough and Thompson, 1977); (c) delamination in the central and northern Sierras (Farmer et al., 2002); (d) mantle drip (Saleeby and Foster, 2004); (e) uniform uplift related to slip on the Owens Valley frontal fault (Wakabayashi and Sawyer, 2001); (f) climate-driven isostatic rebound (Small and Anderson, 1995).

south to the San Joaquin River. One shortcoming of this hypothesis is the lack of datable geomorphic markers south of the San Joaquin River.

Alternatively, Sierran uplift may be in response to the northward migration of the Mendocino triple junction that resulted in crustal thinning in response to an increase in heat flux after the removal of the subducted slab (Crough and Thompson, 1977; Jones et al., 2004). According to this hypothesis, because the triple junction moved from south to north, the southern Sierra have been rising the longest and have therefore experienced the most total uplift (Fig. 2b).

Still another hypothesis proposes that uplift initiated because of westward migration of Basin and Range extension (Niemi, 2003). Extension may be related to delamination of the upper mantle from the lower crust (Ducea and Saleeby, 1998; Liu and Shen, 1998; Manley et al., 2000; Niemi, 2003). Once the lower crust delaminated and sank into the mantle, rising asthenosphere induced uplift (Ducea and Saleeby, 1998; Liu and Shen, 1998). Because Basin and Range extension propagated to the NW over time (Reheis and Dixon, 1996; Monastero et al., 2002) and delamination began in the late Miocene or early Pliocene (Manley et al., 2000), the associated uplift would have progressively decreased with time. Assuming this is true, the most recent uplift would be located in the northern Sierras, the last place to experience Basin and Range extension (Fig. 2a).

Delamination may not have occurred in the southernmost Sierras near the Kern, Kaweah, and Tule Rivers, but rather in northerly parts of the range. This hypothesis is based, in part, on the absence of high potassium Pliocene volcanism associated with delamination in the Kern Volcanic Field in the southern Sierra (Farmer et al., 2002). This hypothesis predicts that the least amount of tectonic activity would be found in the south-central Sierras (Fig. 2c). Furthermore, the effects of Pliocene delamination in the northern and central Sierras would have decreased throughout the Quaternary as the crust rebounds. This decrease in uplift rate during the Quaternary has been observed in the Sierras (Stock et al., 2004).

The Pliocene delamination and subsequent mantle instability would have generated a mantle drip structure (Fig. 1) in the mantle below the Tulare Basin (Saleeby and Foster, 2004). This mantle drip may be pulling down the crust near the Kings, Kaweah, and Tule Rivers (Fig. 2d), generating a basin in this region of the San Joaquin Valley.

Another hypothesis infers that tilting of the Sierras may be in response to isostatic rebound from high rates of glacial erosion (Montgomery, 1994; Small and Anderson, 1995). According to Small and Anderson (1995), this hypothesis predicts that the greatest amounts of denudation, and therefore isostatic response, occurred in areas with the greatest glaciation. The formation of glaciers depends on elevation and the rate of precipitation. The highest elevations are found in the central Sierra (Fig. 3). Sierra precipitation varies more with elevation than with latitude, but precipitation is higher in the northern Sierras (Fig. 1). As a result, the southernmost Sierra near the Kern River would have had the least glaciation as it has lower elevations and precipitation and, consequently, relatively lower uplift rates (Fig. 1G).

The main data sets previously used to evaluate these different hypotheses is river incision (Huber, 1981; Wakabayashi and Sawyer, 2001; Stock et al., 2004). However, as mentioned above, incision rates are limited to the area north of the Kings River because datable deposits are not found within the Kaweah, Tule, and Kern drainages (Wakabayashi and Sawyer, 2001; Stock et al., 2004). Likewise, the detailed study of tilted strata in the San Joaquin Valley is limited to the region between the Kings and Feather Rivers (Unruh, 1991). Geomorphic indices can be used along the entire range since there are no data constraints.

3. Methods

3.1. Base maps

Digital elevation models (DEMs) were used to calculate geomorphic indices. Whenever possible, 10-m DEMs were used instead of the

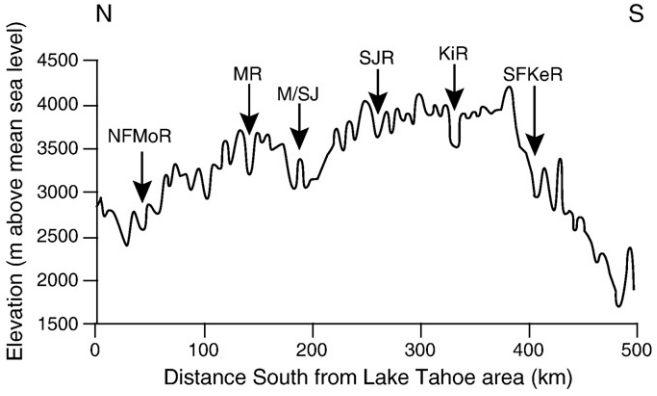

Fig. 3. Sierra Nevada range-crest profile. Key topographic features are the North Fork of the Mokelumne River (NFMoR); Merced River (MR); Merced and San Joaquin River drainage divide (M/SJ); San Joaquin River (SJR); King River (KiR); and South Fork of the Kern River (SFKeR). Location of profile is shown on Fig. 1.

lower resolution 90-m DEMs. The 90-m DEMs cause artificial decreases in the measurements of slopes and channel lengths (Finlayson and Montgomery, 2003). In a few locations, 10-m DEMs are not available and 30-m DEMs were used in their place. The measurement of mountain front sinuosity was made using 90-m DEMs. All river length measurements were made using Rivertools, as were all river longitudinal profiles. Mapinfo v 7.0 was used in the measurement and calculation of all other values (Table 1).

3.2. Tectonic geomorphic indices

Tectonic activity induces topographic and base-level changes in fluvial systems that may be used to decipher relative tectonic activity among mountain ranges (e.g., Bull and McFadden, 1977) and segmentation along a single mountain range (e.g., Wells et al., 1988). Quantification of geomorphic response to tectonic activity may be done by using geomorphic indices (Bull, 1984). Geomorphic indices applicable to fluvial systems in different regions, and of varying size (Strahler, 1958), correlate with independently derived uplift rates (Kirby and Whipple, 2001; Merritts and Vincent, 1989; Rockwell et al., 1985) and are applicable to a variety of tectonic settings where topography is being changed (Azor et al., 2002; Bull and McFadden, 1977; Wells et al., 1988). Bull and McFadden (1977) showed that geomorphic indices applied to half grabens in the Basin and Range clearly discriminate between the active and inactive sides of a range.

3.2.1. Mountain front sinuosity

Mountain front sinuosity (Table 1) is the ratio of the distance along the mountain front at the mountain front piedmont intersection over the straight line distance of the same mountain front (Bull and McFadden, 1977). The mountain front sinuosity was calculated along different segments of the mountain front that have the same strike. Rivers debouching along a fault-bounded, actively uplifting mountain front have little time to laterally erode, yielding a linear mountain front with sparse embayments. The less active the mountain front, the greater the amount of lateral erosion and embayment of the mountain front-piedmont intersection. Thus, a tectonically active mountain front will have a mountain front sinuosity (MFS) value close to 1, whereas an inactive mountain front may have values as high as 7 (Bull and McFadden, 1977).

3.2.2. Valley floor width-to-height ratio

Valley floor width to valley height ratio is calculated (Table 1) 1 km upstream from the mountain front as the width of the valley floor divided by the average height of the valley divides (Bull and McFadden, 1977; Rockwell et al., 1985; Wells et al., 1988). This index quantifies the observation that V-shaped valleys are formed in more tectonically active areas, whereas U-shaped valleys are formed in less active settings. More tectonically active mountain fronts will have V-shaped valleys and very low ratios because they will have steeply incised gorges with high relief and narrow valleys (Bull and McFadden, 1977).

Table 1
Summary and explanation of morphometric parameters used in tectonic landform analysis (after Wells et al., 1988).

Morphometric index	Mathematical derivation	Measurement procedure
Mountain front sinuosity	$\frac{Lmf}{Ls}$	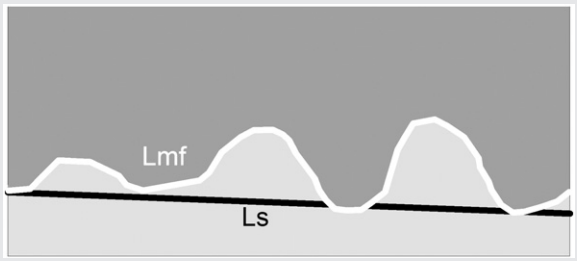
Valley floor width to height ratio	Lfw $[(El-Es)+(Er-Es)]/2$	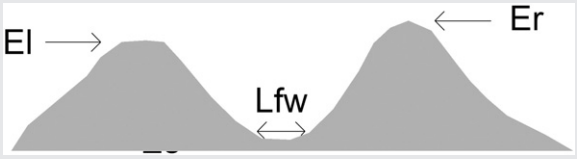
Relief ratio	$\frac{Lr}{Ed-Ev}$	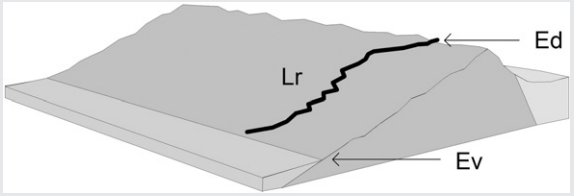
Concavity	Ac At	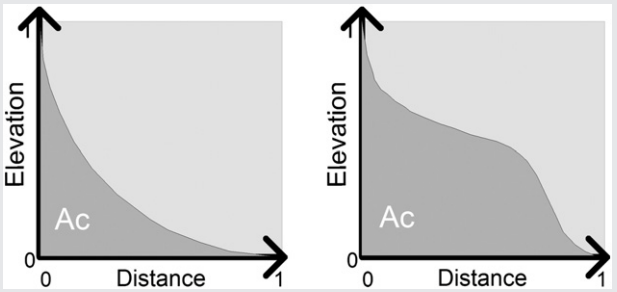

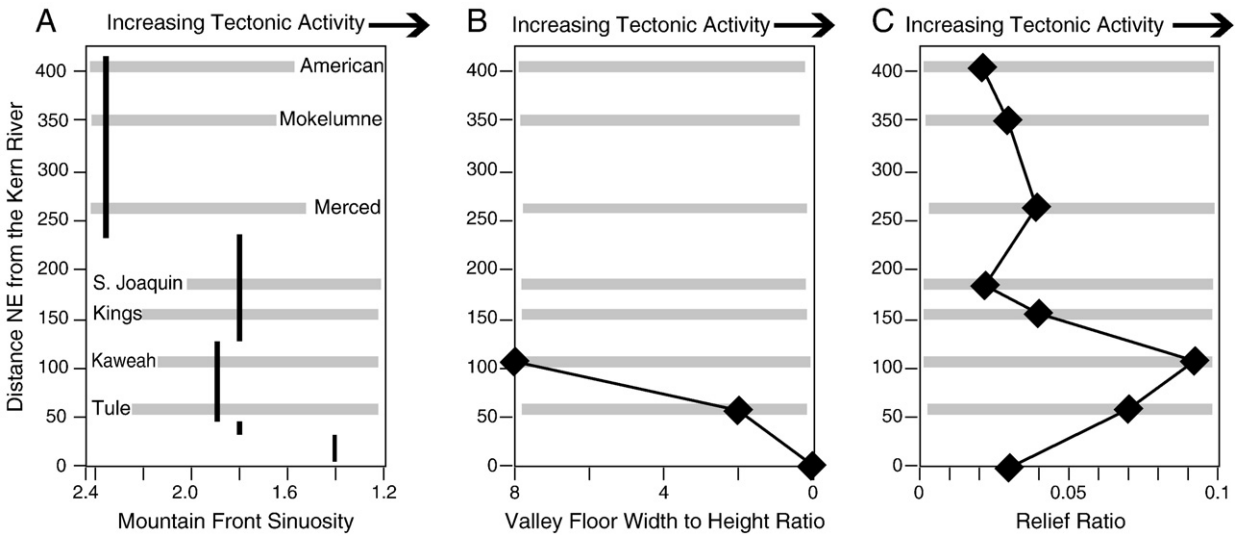

Fig. 4. Plots of (A) mountain front sinuosity, (B) valley floor width to height ratio and (C) relief ratio versus distance NE of the Kern River. Gray bars indicate rivers shown on Fig. 1 and as labeled on A.

3.2.3. Relief ratio

The relief ratio measures the average gradient of a river (Table 1). It is calculated as the basin relief divided by the stream length (Strahler, 1958). When a large river is uplifted, the higher order streams (near the mouth of the river) will have enough stream power to incise into bedrock, thereby lowering to the new base level. This incision will increase the relief of the basin without increasing the length of the river, so that the overall gradient of the river increases.

3.2.4. Longitudinal profiles of trunk streams

The gradients and longitudinal profiles of rivers have been extensively used to interpret tectonic history (Wells et al., 1988; Merritts and Vincent, 1989; Kirby and Whipple, 2001; Mayer et al., 2003; Snyder et al., 2003; Schoenbohm et al., 2004). River profiles record long-term system equilibrium (Ritter et al., 2002). Longitudinal profiles of rivers show tectonic activity through their overall morphology and knickpoints in locations where there is a rapid change in river gradient. Rivers in equilibrium have a concave upward shape where higher order streams have lower gradients than lower order streams (Keller and Pinter, 2002). Rivers in uplifting mountain belts are in disequilibrium and may have a convex upward shape. The convex upward shape is only maintained until the river is able to incise the convex upward part of the profile. Because the highest order streams have the greatest stream power, these streams are more likely to reach equilibrium faster (Burbank and Anderson, 2001).

Faults that cross the stream's profile will create a deviation from the concave upwards longitudinal profile. To regain equilibrium, the knickpoint (a location with a large change in gradient) will migrate upstream through the profile. Downstream from the knickpoint is the newly incised area and upstream is the former equilibrium gradient of the river. The location of knickpoints has been used to infer tectonic activity (Merritts and Vincent, 1989; Monastero et al., 2002; Hodges et al., 2004; Schoenbohm et al., 2004) and amount of uplift (Hodges et al., 2004).

3.2.5. Longitudinal profiles of tributaries

Most longitudinal profile studies focus on the trunk streams; however, tributaries may add insight because their lower stream power results in a slower return to equilibrium profile than the trunk stream (Snyder et al., 2003). In areas where the trunk stream has a convex profile and no knickpoints, tributaries with knickpoints may be used to interpret past tectonic activity (Schoenbohm et al., 2004).

3.2.6. Concavity of tributaries

The concavity index is used to quantify the longitudinal profile morphology (Wells et al., 1988; Kirby and Whipple, 2001). The concavity index is the area under the normalized stream profile (Table 1; Wells et al., 1988). The elevation is normalized by dividing the elevation at a given location by the total basin relief. The distance is normalized by dividing the distance of any given point downstream by the total distance from divide to the confluence between the tributary and trunk stream. The fraction of area under the curve is then calculated. Equilibrium profiles will have a lower concavity index, whereas rivers in tectonically active regions will have higher concavity indices (Table 1).

4. Results

4.1. Mountain front sinuosity

In the southern Sierra near the Kern River, the mountain front sinuosity is 1.4 (Fig. 4). North of the Kern River, the mountain front sinuosity increases to 1.8. Near the Merced, Mokelumne, and American Rivers the mountain front sinuosity increases again to 2.3.

4.2. Valley floor width-to-height ratio

A series of dams have been constructed within 1 km of the mountain front, thus preventing determination of valley floor width-to-height ratios on all but three rivers in the southern portion of the Sierra. Valley floor width-to-height ratios ranged from 0.1 (Kern River) to 8 (Kaweah River) (Table 2 and Fig. 4B).

Table 2
Valley floor height-to-width ratios.

River	Valley floor height-to-width ratio
Kern	0.1
Tule	2.0
Kaweah	8.0
Kings	Dammed
San Joaquin	Dammed
Merced	Dammed
Mokelumne	Dammed
American	Dammed

Table 3
Relief ratios for Sierra Nevada Rivers: rivers are listed from southernmost (Kern) to northernmost (American).

River	Relief ratio
Kern	0.03
Tule	0.07
Kaweah	0.09
Kings	0.04
San Joaquin	0.02
Merced	0.04
Mokelumne	0.03
American	0.02

4.3. Relief ratio

The relief ratios of the large river drainage basins vary from 0.7 to 0.2 (Table 3). The highest relief ratios are 0.07 and 0.09 for the Tule and Kaweah Rivers, respectively (Fig. 4C). All the other rivers north of the Kaweah River have relief ratios of are 0.04 or greater.

4.4. Longitude profiles of trunk streams

Two longitudinal profiles were extracted along channels in the Kern River drainage. The main fork of the Kern River (Fig. 5A) is fault controlled above Lake Isabella (Webb, 1955; Nadin and Saleeby, 2010). A profile of the westward-flowing Kern River tributary Sweetwater Creek (Fig. 5B) was also drawn. Both longitudinal profiles show a prominent convex upward section of the profile at the mountain front. Upstream from the convex upward section both profiles have a relatively concave upward shape, showing that at least 600 m of incision in the lower reaches.

The Tule River has an overall concave upward shape (Fig. 6A). A knickpoint indicates at least 200 m of incision has occurred near the mouth of the river. The Kaweah River also has a concave upward longitudinal profile (Fig. 6B), but a knickpoint is found at the confluence with a tributary, showing that the river is not completely in equilibrium. The Kaweah River knickpoint is at an elevation of 2000 m within the glaciated portion of the Sierra.

The Kings River has an overall concave upward profile, but several knickpoints are found at the confluence between tributaries and the trunk streams in both the middle and south forks and at the confluence between the two forks (Fig. 6C). The one knickpoint with a low enough elevation to rule out as glacial in origin shows at least 200 m of incision. The San Joaquin longitudinal profile does not have a concave upward longitudinal profile (Fig. 7A). The profile is partly a result of three reservoirs along the river's course. These reservoirs make the interpretation of the profile difficult.

The Merced River longitudinal profiles are a good example of the effects of glaciation. The main (north) fork of the Merced has several prominent knickpoints that are the result of glacial downcutting near Yosemite Valley (Fig. 7B). The longitudinal profile of the Merced River south fork, however, does not contain these large knickpoints (Fig. 7C). Instead, the south fork has one small knickpoint located near glacial deposits and is therefore likely the result of glacial erosion.

The Mokelumne River has a prominent knickpoint at the confluence between the north and middle forks (Fig. 8A), showing that the river is in disequilibrium. The knickpoint is at such a low elevation that it is unlikely to be the result of glaciation. Because it is found at the confluence between forks in the river, this knickpoint is likely the result of an increase in stream power.

The American River's longitudinal profile has a prominent knickpoint (Fig. 8B) near the contact with resistant granite and near

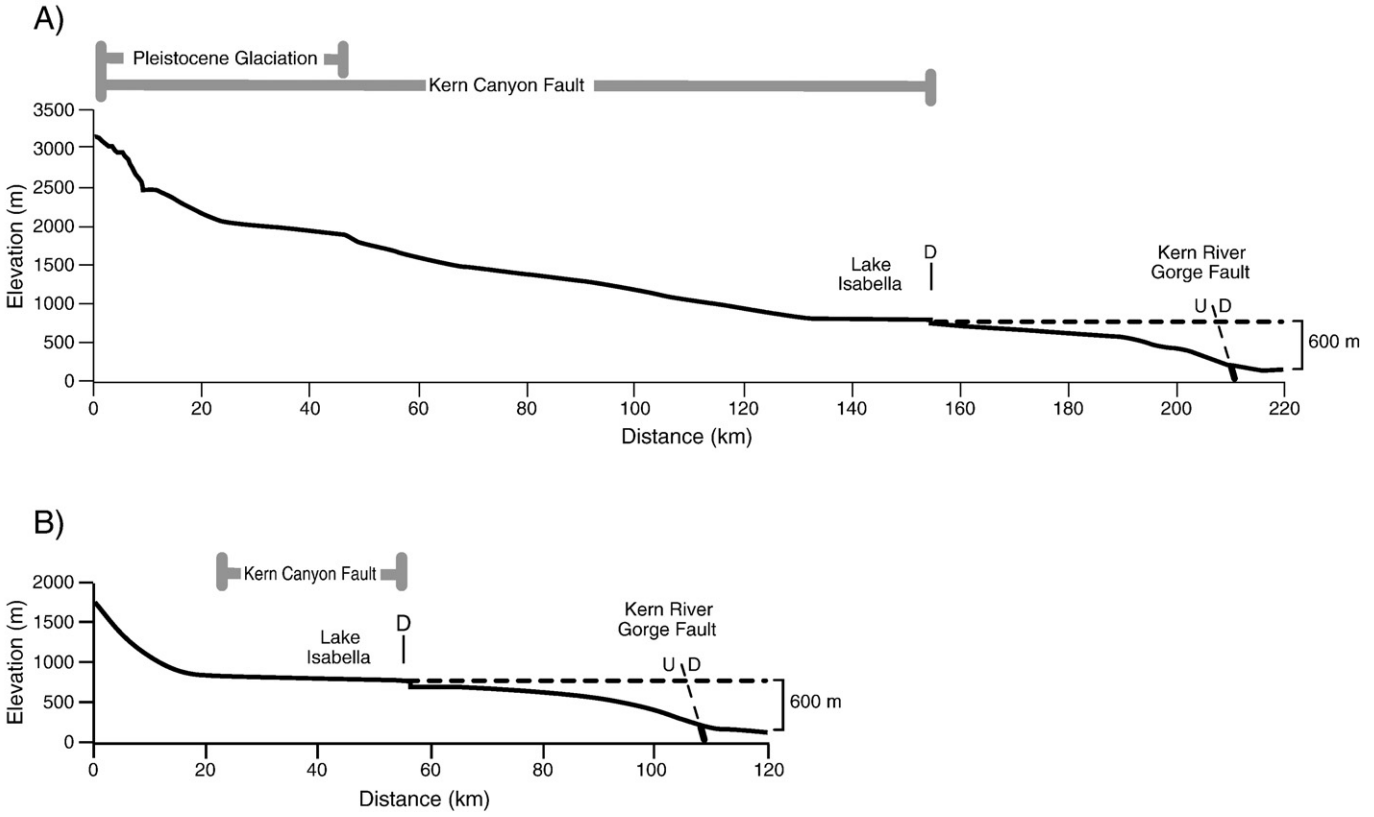

Fig. 5. Longitudinal profiles of the Kern River (A) and its tributary Sweetwater Creek (B). Distances are measured downstream from the basin divide. Gray bars show the lateral extent of Pleistocene glaciation and the Kern Canyon fault. Dam location (D) and relative movement (U = upthrown block; D = downthrown block) of fault are also shown.

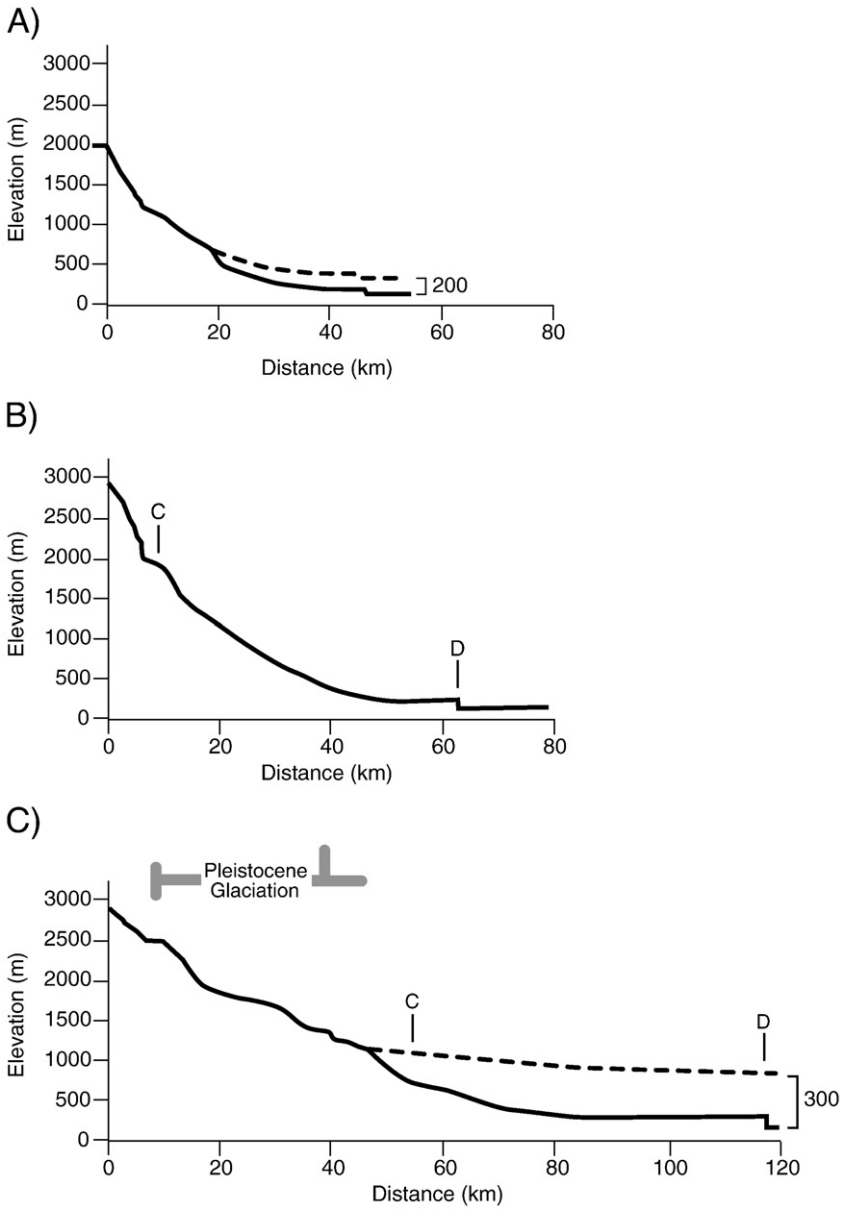

Fig. 6. Longitudinal profiles of the Tule (A), Kaweah (B) and Kings (C) Rivers. Distances are measured downstream from the basin divide. Gray bars show the lateral extent of Pleistocene glaciation. Dam locations (D) and confluences (C) with major tributaries are also shown.

the Silver Creek confluence. Either the lithology change or confluence could cause the gradient change. The low elevation suggests that the knickpoint is unlikely the result of glacial erosion. The knickpoint shows 400 m of incision (Table 4).

4.5. Concavity of tributaries

To further resolve the areas of greatest tectonic activity, normalized longitudinal profiles of tributaries were drawn. These tributaries were one order lower than the trunk stream (Strahler, 1958). The Merced, Mokelumne, San Joaquin, and Kings Rivers have tributaries that are all a similar distance from the mountain front (Fig. 9) but have widely ranging concavities of 0.51, 0.41, 0.32, 0.26, respectively. Similarly, the Kern, Kaweah, and Tule Rivers all have tributaries that are about the same distance from the mountain front (Fig. 9). The Kern River tributary has the higher concavity (0.49) compared with the tributaries of the Tule (0.32) and Kaweah (0.39).

5. Discussion

5.1. Interpretation of geomorphic indices

5.1.1. Mountain front sinuosity

Bull and McFadden (1977) classified mountain fronts with sinuosities <2 as tectonically active (Class 1 or 2). Along the so-called inactive or passive western Sierra mountain front, the mountain front sinuosity south of the Merced River is <2. The lowest mountain front sinuosity value (1.3) was found in the southernmost area near the Kern River indicating that the greatest tectonic activity is in the southernmost Sierra.

From the Tule River north to near the Merced River, the mountain front sinuosity is 1.8–1.9. This class 2, active mountain front coincides with anomalous topography (more linear mountain front) and the mantle drip (Fig. 1) related to Pliocene crustal delamination (Saleeby and Foster, 2004). This area also includes the Kings River mouth as well that Stock et al. (2004) described the Kings River basin as

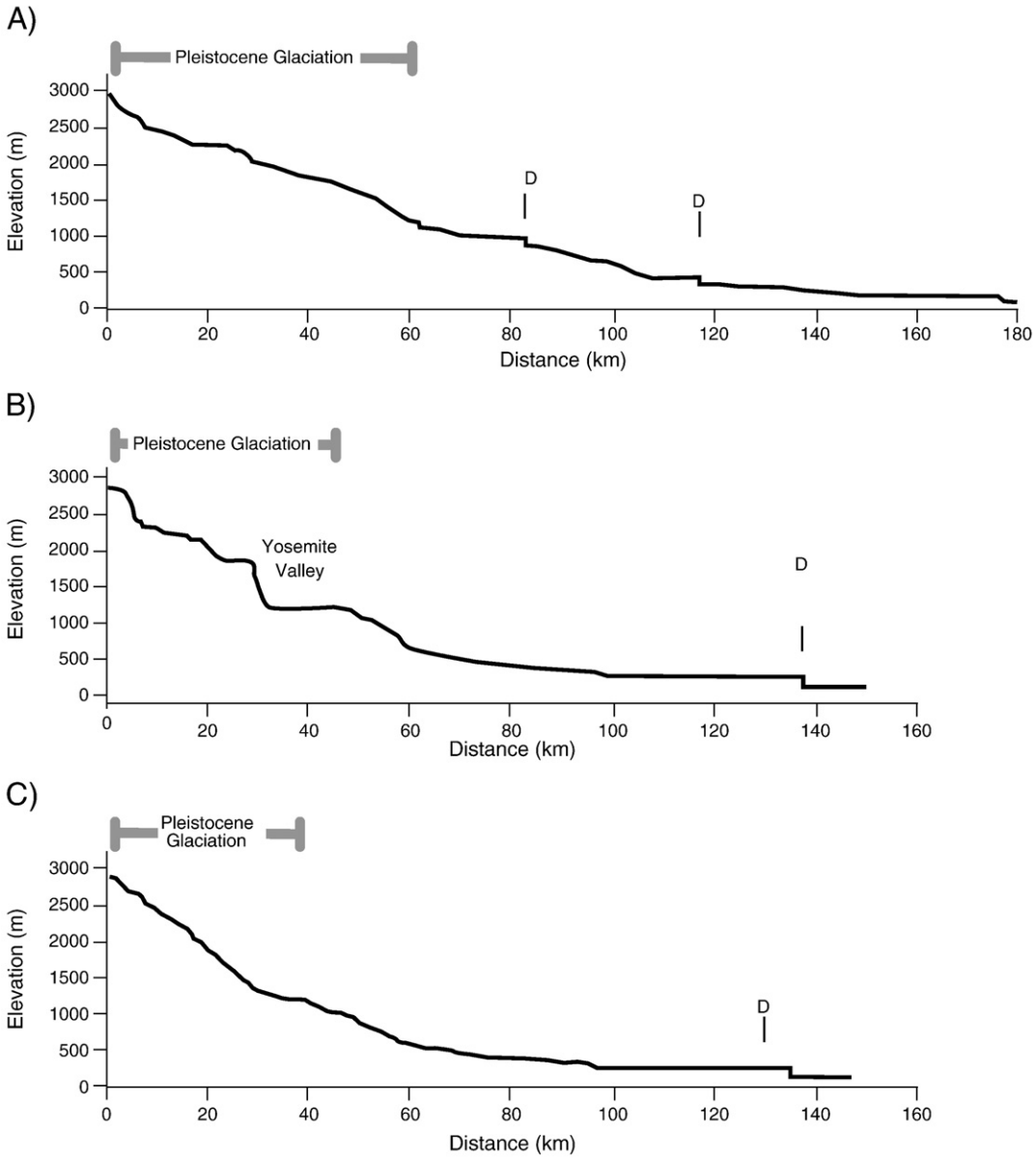

Fig. 7. Longitudinal profiles of the San Joaquin (A), Merced (B) and Merced-south fork (C) Rivers. Distances are measured downstream from the basin divide. Gray bars show the lateral extent of Pleistocene glaciation. Dam locations (D) are also shown.

experiencing post-Pliocene incision, possibly related to the Pliocene crustal delamination. North of the Merced River, the mountain front sinuosity values are 2.4 suggesting an inactive mountain front (Bull and McFadden, 1977; Bull, 1984).

5.1.2. Valley floor width-to-height ratio

Although the data is limited, the high valley floor width-to-height ratio of the Kern River shows a high degree of tectonic activity within the range that Bull and McFadden (1977) classified as tectonically active. Rockwell et al. (1985) found that mountain fronts with a tectonic activity class of 1 and similar valley floor height-to-width ratios and mountain front sinuosity had uplift rates of 0.4 to 2–8 mm/y. This broad range overlaps with uplift rates for faults along the eastern Sierra where geologic slip rates range from 0.1–2.5 mm/yr (e.g., Zehfuss et al., 2001; Le et al., 2007) and the overall late Cenozoic uplift estimates of 0.2–0.4 mm/yr for the Sierra (Huber, 1981; Graham et al., 1988; Unruh, 1991; Wakabayashi and Sawyer, 2001; Clark et al., 2005).

5.1.3. Relief ratio

Relief ratios indicate that the southern Sierras (near the Tule, Kaweah, and Kings Rivers) are more tectonically active than the northern Sierras (Fig. 4C). The Kern River has a low relief ratio, like the northern rivers, suggesting that it too may have a lesser amount of tectonic activity; however, the interpretation of relief is complicated by the fact that the Kern River does not flow perpendicular to the axis of uplift like all of the other rivers. Upstream from Lake Isabella, the Kern River flows north–south following the Kern Canyon fault (Fig. 1; Webb, 1936; Moore and du Bray, 1978). This structural control on the upper reaches of the Kern River limits the reliability of relief ratio as an indicator of tectonic activity.

5.1.4. Longitudinal profiles of trunk streams

All rivers on the western side of the Sierras have concave upward profiles with few or small knickpoints, except for the Kern River (Fig. 5A). We interpret the convex upward shape of the Kern River profile at the mountain front to show that this is an area of rapid base level change near the mountain front. Because the Kern Gorge fault is

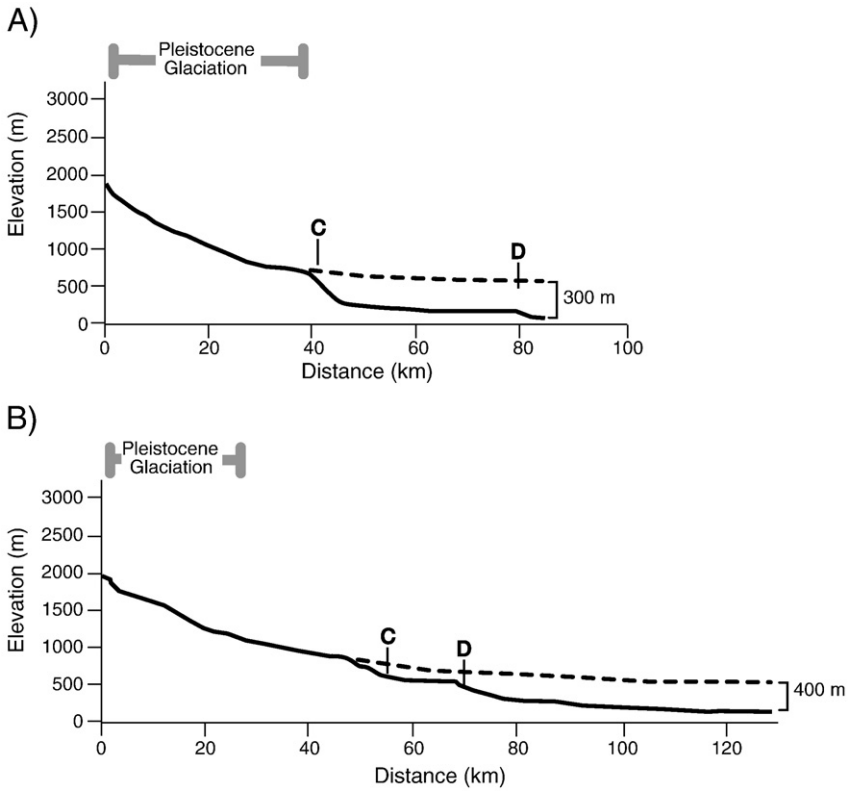

Fig. 8. Longitudinal profiles of the Mokelumne (A) and American (B) Rivers. Distances are measured downstream from the basin divide. Gray bars show the lateral extent of Pleistocene glaciation. Dam locations (D) and confluences (C) with major tributaries are also shown.

located at the mountain front and the longitudinal profile shows at least 600 m of vertical uplift of the basement (Hart et al., 1984), we infer that slip on the Kern Gorge fault is the likely cause of the convex shape of the profile. If 600 m of uplift at the mountain front is subtracted from the longitudinal profile (Fig. 5A), the old mountain front may have been located at the elevation of Lake Isabella and the Kern River may have been in equilibrium, with a convex profile, prior to a recent pulse of uplift at the mountain front.

The Tule, Kings, and American Rivers also have knickpoints in their longitudinal profiles that cannot be easily related to glaciation. We interpret these knickpoints to be evidence of Quaternary tectonic activity along the mountain front.

5.1.5. Concavity of tributaries

Tributaries closest to the mouth of the river would show response to tectonism more quickly as the knickpoint migrates from the mouth upstream. In addition, tributaries closest to the river mouth are less likely affected by glacial erosion at these lower elevations. The position relative to the river mouth is clearly demonstrated by two tributaries of the San Joaquin River (Fig. 9). Therefore, we compare concavity of tributaries that are the same distance from the mountain front.

The concavity of tributaries suggests tectonic activity in two locations within the range. Dividing the tributary concavities by distance from river mouth, the Merced, Mokelumne, San Joaquin, and Kings Rivers all have tributaries that are approximately the same distance from the mountain front but have varying concavities. The Merced and Mokelumne have higher concavities, suggesting that knickpoints have not migrated upstream and have had more recent uplift than the San Joaquin and Kings Rivers.

Similarly, the Kern, Kaweah, and Tule Rivers all have tributaries that are approximately the same distance from the mountain front. The Kern River has a higher concavity than the Kaweah and Tule Rivers, which is interpreted as a greater rate of tectonic activity.

Table 4
Concavity index of tributaries near the mouth of each river.

Tributary	Concavity
Kern River	0.49
Tule	0.32
Kaweah	0.39
Kings	0.26
San Joaquin	0.32
Merced	0.51
Mokelumne	0.41
American	0.19[a]

[a] Concavity is greatly affected by damming at the mountain front.

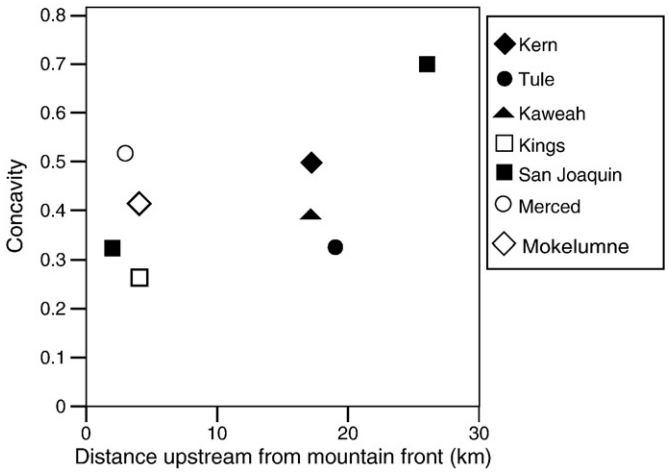

Fig. 9. Plot of stream concavity versus distance upstream from mountain front.

5.2. Summary of tectonic geomorphology

Variations in the geomorphic indices along the western Sierra suggest different uplift histories and base level changes in different areas. The geomorphic indices show higher tectonic activity in two regions of the Sierras. High tectonic activity (either greatest magnitude or most recent uplift) is found in the southern Sierras (i) near the Kaweah and Tule Rivers and (ii) near the Kern River mouth where the greatest activity is found. Although not as prominent, relatively greater tectonic activity is found in the northernmost Sierras (near the American and Mokelumne Rivers) compared to the central Sierras (Fig. 10). Greater tectonic activity in the northern Sierra is coincident with the Melones and Bear Mountain fault zones.

Several of the hypothesized mechanisms for uplift do not fit with the observed geomorphology. The lower valley floor width-to-height ratios, higher relief ratios, and low mountain front sinuosity are interpreted to show greater tectonic activity in the southern Sierra (Fig. 10). Therefore, the hypotheses that predict block uplift of the Sierra (Fig. 2e), delamination from Basin and Range extension (Fig. 2b), and delamination of the northern and central Sierras (Fig. 2c) do not fit the observed geomorphology. The mantle drip (Fig. 2d) and isostatic rebound (Fig. 2f) hypotheses explain the higher tectonic activity near the Kaweah and Tule Rivers, but do not fit the observation that the greatest tectonic activity is found near the Kern River. Westward migration of the Basin and Range extension predicts that the greatest amount of uplift will be in the Kern River region (Fig. 1B); however, Basin and Range extension in the southern Sierra does not support uplift to the north at the Kings River area as documented by Stock et al. (2004).

Because none of the previously proposed hypotheses fits all the data, we propose an alternative, hybrid, two-stage hypothesis for late Cenozoic uplift of the Sierra. We hypothesize that the Pliocene delamination and formation of the mantle drip generated rapid uplift in the Kings River region (Fig. 1; Saleeby and Foster, 2004). The isostatic response to delamination caused relatively rapid uplift of this region and subsequently uplift rates have decreased (Saleeby and Foster, 2004; Stock et al., 2004). A pulse of uplift in the Pliocene accounts for the more linear mountain front (anomalous topography of Saleeby and Foster, 2004) at the Kings River.

The southern Sierra is bounded by the Big Bend region where the greatest obliquity exists between the Pacific-North American plate motion and the trend of the San Andreas Fault (Spotila et al., 2007). Here, we hypothesize that the interactions between the San Andreas, Garlock and Sierra Nevada Frontal faults are driving uplift and tilting of the Sierra. Compression related to the Big Bend in the Sierra and formation of the Transverse Ranges is coincident with the southern Sierra (Spotila et al., 2007). In addition, stress modeling indicates that slip during San Andreas earthquakes may increase stress and promote earthquakes on related faults such as the White Wolf fault (Lin and Stein, 2004).

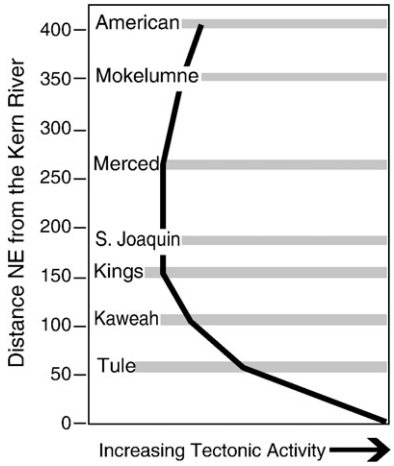

Fig. 10. Summation of relative tectonic geomorphology with distance parallel to the mountain range.

Thus, the initiation of slip on the San Andreas and Garlock faults may be related to subsidence and greater tilting in the southern San Joaquin Valley, as compared to the northern San Joaquin Valley. This would generate late Pliocene to Quaternary uplift in the southernmost Sierras, near the Kern, Tule and Kaweah Rivers.

San Andreas-related tectonics, however, does not explain the observation of the rootless nature of the Sierra (Wernicke et al., 1996), the initiation of Sierra uplift ~8 Ma (Graham et al., 1988; Huber, 1981; Unruh, 1991) or the higher range crest near the Kings River region (Fig. 2). These data are more consistent with the delamination/mantle drip hypotheses as is the more linear mountain front in this region.

Considering these complexities, we hypothesize that the Pliocene delamination and mantle drip generated rapid uplift in the Kings River region (Saleeby and Foster, 2004). Isostatic response to delamination was relatively rapid and has since decreased (Saleeby and Foster, 2004; Stock et al., 2004). Subsequently, over the last 5 Ma, San Andreas plate margin tectonics has caused rapid subsidence in the Tulare Basin, causing incision of the lower reaches of the Kern River along the Kern Gorge Fault. This combination of mechanisms is consistent with the geomorphic indices.

5.3. Limitations on the interpretation of tectonic geomorphology

Tectonic activity is not the only factor that causes differential erosion along a mountain front or within a mountain range. Differences in precipitation (Hodges et al., 2004; Montgomery et al., 2001), bedrock type, and glacial history (Brocklehurst and Whipple, 2002; Hallet et al., 1996) all affect erosion rates and uplift as an isostatic response.

Differences in precipitation are not likely to greatly affect erosion rate in the Sierras since most variation in precipitation occurs with elevation (Fig. 3). In addition, variations in precipitation within the Sierras are not correlated with erosion rates (Riebe et al., 2001).

Differences in bedrock type could affect erosion of the Sierras, but is unlikely. South of the Merced River granite is the predominant rock type with a few metamorphic roof pendants (Wahrhaftig, 1965). Intrusive and volcanic rocks are found within the northern and central sections (Slemmons, 1966) and a variety of rock types are found along the mountain front.

Glacial erosion could affect the interpretations of geomorphic indices because alpine glaciers increase mechanical and chemical denudation rates (Hallet et al., 1996) and erode headward and downward faster than rivers (Brocklehurst and Whipple, 2002) and because the Sierras were intermittently glaciated between 2.9 and 3.2 Ma. Glaciers have extended downvalley in the Sierras to elevations as low as 900–1200 m (Bateman and Wahrhaftig, 1966), thus geomorphic indices were calculated at the mountain front where lower elevations would be less affected by glaciation. In addition, gradient changes in longitudinal profiles were evaluated for the possibility that these changes resulted from glacial erosion.

6. Conclusions

A combination of Pliocene lower crust/upper mantle delamination followed by late Pliocene to present San Andreas plate boundary deformation is most consistent with Sierra geomorphology. The delamination and mantle drip hypotheses explain the lack of crustal root in the central Sierras, as well as the higher elevations in the Kings River region. Because delamination occurred in the Pliocene, the effects would wane during the Quaternary. This is consistent with uplift rates in the central and northern Sierras (Stock et al., 2004). The higher tectonic activity in the southwestern Sierras and southern San Joaquin Valley is a consequence of San Andreas, Garlock, and Sierra

Nevada Frontal fault interactions (Figueroa, 2005) beginning in the late Pliocene and continuing to the present.

Acknowledgements

This study was supported by a grant from California State University–Fullerton. Earlier versions of this manuscript benefited from reviews by David Bowman and Phillip Armstrong. Reviews by Kurt Frankel, Lewis Owen and anonymous review along with Richard Marston greatly improved the manuscript.

References

Atwater, B.F., Adam, D.P., Bradbury, J.P., Forester, R.M., Mark, R.K., Lettis, W.R., Fisher, G.R., Gobalet, K.W., Robinson, S.W., 1986. A fan dam for Tulare Lake, California, and implications for the Wisconsin glacial history of the Sierra Nevada. Geological Society of America Bulletin 97, 97–109.

Azor, A., Keller, E.A., Yeats, R.S., 2002. Geomorphic indicators of active fold growth: South Mountain-Oak Ridge anticline, Ventura basin, southern California. Geological Society of America Bulletin 114 (6), 745–753.

Bartow, J.A., 1991. The Cenozoic evolution of the San Joaquin Valley, California. U.S.G.S. Professional Paper 1501,Washington, D.C, pp. D1–D40.

Bateman, P.C., Wahrhaftig, C., 1966. Geology of the Sierra Nevada. In: Bailey, E. (Ed.), Geology of Northern California. California Division of Mines and Geology, Sacramento, CA, pp. 107–172.

Blackwelder, E., 1931. Pleistocene glaciation in the Sierra Nevada and Basin Ranges. Geological Society of America Bulletin 42, 865–922.

Brocklehurst, S.H., Whipple, K.X., 2002. Glacial eroison and relief production in the Eastern Sierra Nevada, California. Geomorphology 42, 1–24.

Bull, W.B., 1984. Tectonic geomorphology. Journal of Geological Education 32, 310–324.

Bull, W.B., McFadden, L.D., 1977. Tectonic geomorphology north and south of the Garlock fault, California. In: Doehring, D.C. (Ed.), Geomorphology in Arid Regions, Proceedings 8th Annual Geomorphology Symposium. State University of New York, Binghamton, NY, pp. 115–137.

Burbank, D.W., Anderson, R.S., 2001. Tectonic geomorphology. Blackwell Science, Malden, MA.

Cecil, M.R., Ducea, M.N., Reiners, P.W., Chase, C.G., 2006. Cenozoic exhumation of the northern Sierra Nevada, Califronia, from (U-Th)/He thermochronology. Geological Society of America Bulletin 118, 1481–1488.

Clark, M.K., Gweltaz, M., Saleeby, J., Farley, K.A., 2005. The non-equilibrium landscape fo the southern Sierra Nevada, California. GSA Today 15, 4–10.

Crough, S.T., Thompson, G.A., 1977. Upper mantle origin of Sierra Nevada uplift. Geology 5, 396–399.

Ducea, M., Saleeby, J.B., 1998. A case for delamination of the deep batholithic crust beneath the Sierra Nevada, California. International Geology Review 40 (1), 78–93.

Dumitru, T.A., 1990. Subnormal Cenozoic geothermal gradients in the extinct Sierra Nevada magmatic arc: consequences of Larmide and post-Laramide shallow-angle subduction. Journal of Geophysical Research 95, 4925–4941.

Farmer, G.L., Glazner, A.F., Manley, C.R., 2002. Did lithospheric delamination trigger late Cenozoic potassic volcanism in the southern Sierra Nevada, California. Geological Society of America Bulletin 114 (6), 754–768.

Figueroa, A.M., 2005. Elastic modeling and tectonic geomorphic investigation of the Late Cenozoic Sierra Nevada (California) uplift. M.S. Thesis, California State University-Fullerton, CA.

Finlayson, D.P., Montgomery, D.R., 2003. Modeling large-scale fluvial erosion in geographic information systems. Geomorphology 53, 147–164.

Graham, S.A., Carroll, A.R., Miller, G.E., 1988. Kern River Formation as a recorder of uplift and glaciation of the southern Sierra Nevada. In: Graham, S.A. (Ed.), Studies of the geology of the San Joaquin basin. Society of Economic Paleontologists and Mineralogists, Los Angeles, CA, pp. 319–332.

Hallet, B., Hunter, L., Bogen, J., 1996. Rates of erosion and sediment evacuation by glaciers: a review of field data and their implications. Global and Planetary Change 12, 213–235.

Hart, E.W., Bryant, W.A., Smith, T.C., 1984. Summary Report: Fault Evaluation Program, 1983 Area (Sierra Nevada Region). California Division of Mines and Geology, Sacramento, CA.

Hodges, K.V., Wobus, C., Ruhl, K., Schildgen, T., Whipple, K., 2004. Quaternary deformation, river steepening, and heavy precipitation at the front of the Higher Himalayan ranges. Earth and Planetary Science Letters 220, 379–389.

House, M.A., Wernicke, B.P., Farley, K.A., Dumitru, T.A., 1997. Cenozoic thermal evolution of the central Sierra Nevada, California from (U-Th)/He thermochronometry. Earth and Planetary Science Letters 151, 167–179.

House, M.A., Wernicke, B.P., Farley, K.A., 1998. Dating topography of the Sierra Nevada, California, using apatite (U-Th)/He ages. Nature 396, 66–69.

House, M.A., Wernicke, B.P., Farley, K.A., 2001. Paleogeomorphology of the Sierra Nevada, California from the (U-Th)/He ages in apatite. American Journal of Science 301, 77–102.

Huber, N.K., 1981. Amount and timing of Late Cenozoic uplift and tilt of the Central Sierra Nevada, California—evidence from the upper San Joaquin River Basin. U.S. Geological Survey Professional Paper 1197, Washington, D.C, pp. 1–28.

Jones, C.H., Farmer, G.L., Unruh, J., 2004. Tectonics of Pliocene removal of lithosphere of the Sierra Nevada, California. Geological Society of America Bulletin 116 (11/12), 1408–1422.

Keller, E.A., Pinter, N., 2002. Active tectonics: earthquakes. Uplift and Landscape, Prentice Hall, Upper Saddle River, NJ.

Kirby, E., Whipple, K., 2001. Quantifying differential rock-uplift rates via stream profile anaylsis. Geology 29 (5), 415–418.

Le, K., Lee, J., Owen, L.A., Finkel, R., 2007. Late Quaternary slip rates along the Sierra Nevada frontal fault zone, California: slip partitioning across the western margin of the Eastern California Shear Zone - Basin and Range Province. Geological Society of America Bulletin 119 (1/2), 240–256.

Lin, J., Stein, R., 2004. Stress triggering in thrust and subduction earthquakes and stress interaction between the southern San Andreas and nearby thrust and strike-slip faults. Journal of Geophysical Research-Solid Earth 109 (B2). doi:10.1029/2003JB002607.

Liu, M., Shen, Y., 1998. Sierra Nevada uplift: a ductile link to mantle upwelling under the Basin and Range province. Geology 26 (4), 299–302.

Manley, C.R., Glazner, A.F., Farmer, G.L., 2000. Timing of volcanism in the Sierra Nevada of California: evidence for Pliocene delamination of the batholithic root? Geology 28 (9), 811–814.

Mayer, L., Menichetti, O., Nesci, O., Savelli, D., 2003. Morphotectonic appraoch to the drainage analysis in the North Marche region, central Italy. Quaternary International 101–102, 157–167.

Merritts, D.J., Vincent, K.R., 1989. Geomorphic response of coastal streams to low, intermediate, and high rates of uplift, Mendocino triple junction region, northern California. Geological Society of America Bulletin 101 (11), 1373–1388.

Monastero, F.C., Walker, J.D., Katzenstein, A.M., Sabin, A.E., 2002. Neogene evolution of the Indian Wells Valley, east-central California. In: Glazner, A.F., Walker, J.D., Bartley, J.M. (Eds.), Geologic Evolution of the Mojave Desert and Southwestern Basin and Range. Geological Society of America Memoir 195, Boulder, CO, pp. 199–228.

Montgomery, D.R., 1994 Valley incision and the uplift of mountain peaks. Journal of Geophysical Research 99(B7), 13,913-13,921.

Montgomery, D.R., Balco, G., Willett, S.D., 2001. Climate, tectonics, and the morphology of the Andes. Geology 29 (7), 579–582.

Moore, J.G., du Bray, E., 1978. Mapped offset on the right-lateral Kern Canyon fault, southern Sierra Nevada, California. Geology 6, 205–208.

Nadin, E., Saleeby, J., 2010. Quaternary reactivation of the Kern Canyon fault system, southern Sierra Nevada, California. Geological Society of America Bulletin 122 (9/10), 1671–1685.

National Atlas of the United States, 2010. http://www.nationalatlas.gov/printable/images/pdf/precip/pageprecip_ca3.pdf.

Niemi, N.A., 2003. Active faulting in the southern Sierra Nevada: initiation of a new Basin and Range normal fault? Geological Society of America Abstracts with Program 35 (6), 581.

Poage, M.A., Chamberlain, C.P., 2002. Stable isotopic evidence for a pre-middle Miocene rain shadow in the western Basin and Range: implications for the paleotopography of the Sierra Nevada. Tectonics 21 (4), 1–10.

Reheis, M.C., Dixon, T.H., 1996. Kinematics of the eastern California shear zone: evidence for slip transfer from Owens and Saline Valley fault zones to Fish Lake Valley fault zone. Geology 24 (4), 339–342.

Riebe, C.S., Kirchner, J.W., Granger, D.E., Finkel, R.C., 2001. Minimal climatic control on erosion rate in the Sierra Nevada, California. Geology 29 (5), 447–450.

Ritter, D.F., Kochel, R.C., Miller, J.R., 2002. Process Geomorphology. Waveland Press, Long Grove, IL.

Rockwell, T.K., Keller, E.A., Johnson, D.L., 1985. Tectonic geomorphology of alluvial fans and mountain fronts near Ventura, California. In: Morisawa, M., Hack, J.T. (Eds.), Binghampton Symposia in Geomorphology International Series, NY: Tectonic geomorphology, pp. 183–207.

Saleeby, J., Foster, Z., 2004. Topographic response to mantle lithosphere removal in the southern Sierra Nevada region, California. Geology 32 (3), 245–248.

Schoenbohm, L.M., Whipple, K.X., Burchfiel, B.C., Chen, L., 2004. Geomorphic constraints on surface uplift, exhumation, and plateau growth in the Red River region, Yunnan Province, China. Geological Society of America Bulletin 116 (7/8), 895–909.

Slemmons, D.B., 1966. Cenozoic volcanism of the central Sierra Nevada, California. In: Bailey, E. (Ed.), Geology of Northern California. California Division of Mines and Geology, Sacramento, CA, pp. 199–208.

Small, E.E., Anderson, R.S., 1995. Geomorphically driven Late Cenozoic rock uplift in the Sierra Nevada, California. Science 270, 277–280.

Snyder, N.P., Whipple, K.X., Tucker, G.E., Merritts, D.J., 2003. Channel response to tectonic forcing: field analysis of stream morphology and hydrology in the Mendocino triple junction region, northern California. Geomorphology 53, 97–127.

Spotila, J.A., Niemi, N., Brady, R., House, M., Buscher, J., Oskin, M., 2007. Long-term continental deformation associated with transpressive plate motion: the San Andreas fault. Geology 35 (11), 967–970.

Stock, G.M., Anderson, R.S., Finkel, R.C., 2004. Pace of landscape evolution in the Sierra Nevada, California revealed by cosmogenic dating of cave sediments. Geology 32 (3), 193–196.

Strahler, A.N., 1958. Dimensional analysis applied to fluvially eroded landforms. Geological Society of America Bulletin 69 (3), 279–299.

Unruh, J.R., 1991. The uplift of the Sierra Nevada and implications for the late Cenozoic epeirogeny in the western Cordillera. Geological Society of America Bulletin 103, 1395–1404.

Wahrhaftig, C., 1965. Stepped topography of the southern Sierra Nevada, California. Geological Society of America Bulletin 76, 1165–1190.

Wakabayashi, J., Sawyer, T.L., 2001. Stream incision, tectonics, uplift and evolution of topography of the Sierra Nevada, California. Journal of Geology 109, 539–562.

Webb, R.W., 1936. Kern Canyon fault, southern Sierra Nevada. Journal of Geology 44 (5), 631–638.
Webb, R.W., 1955. Kern Canyon lineament. In: Oakeshott, G.B. (Ed.), Earthquakes in Kern County, California, during 1952. California Division of Mines and Geology Bulletin, 171, pp. 35–36.
Wells, S.G., Bullar, T.F., Menges, C.M., Drake, P.G., Kara, P.A., Kelson, K.I., Ritter, J.B., Wesling, J.R., 1988. Regional variations in tectonic geomorphology along a segmented convergent plate boundary, Pacific coast of Costa Rica. Geomorphology 1, 239–365.
Wernicke, B.P., Clayton, R., Ducea, M., Jones, C.H., Park, S., Rupper, S., Saleeby, J., Snow, J.K., Squires, L., Fliedner, M., Jiracek, G., Keller, R., Klemperer, S., Luetgert, J., Malin, P., Miller, K., Mooney, W., Oliver, H., Phinney, R., 1996. Origin of high mountains in the continents: the southern Sierra Nevada. Science 271, 190–193.
Zehfuss, P.H., Bierman, P.R., Gillespie, A.R., Burke, R.M., Caffee, M.W., 2001. Slip rates on the Fish Springs fault, Owens Valley, California, deduced from cosmogenic 10Be and 26Al and soil development on fan surfaces. Geological Society of America Bulletin 113 (2), 241–255.